Polyhedral Vanadium Oxide Cages:

Infrared Spectra of Cluster Anions and Size-Induced d-Electron Localization**

Knut R. Asmis*, Gabriele Santambrogio, Mathias Brümmer, Joachim Sauer*

(*)- Dr. K.R. Asmis, Fritz-Haber-Institut der Max-Planck-Gesellschaft, Faradayweg 4-6, D-14195 Berlin, Germany. Tel: +(49)(30)8413-5735, Fax: +(49)(30)8413-5603, E-mail: asmis@fhi-berlin.mpg.de

Dipl. Phys. G. Santambrogio, Dipl. Ing. M. Brümmer, Institut für Experimentalphysik, Freie Universität Berlin, Arnimallee 14, D-14195 Berlin, Germany.

(*)- Prof. Dr. J. Sauer, Institut für Chemie, Humboldt-Universität Berlin, Unter den Linden 6, D-10099, Berlin, Germany. Tel: +(49)(30)2093-7134, Fax: +(49)(30)2093-7136, E-mail: js@chemie.hu-berlin.de

(**) This work has been supported by German Research Foundation DFG as part of the Collaborative Research Center 546. We gratefully acknowledge the support of the “Stichting voor Fundamenteel Onderzoek der Materie (FOM)” in providing the required beam time on FELIX and highly appreciate the skillful assistance of the FELIX staff. We thank L. Wöste and G. Meijer for their continuous support and A. Fielicke for helpful discussions.

The size-dependent properties of transition metal oxide clusters are intensely studied not only because of interest in this peculiar state of matter, but also because of their relevance as building blocks for nanostructured materials. Vanadium oxides, in particular, are important in supported catalysts,[1] as cathode materials in lithium batteries,[2] in bolometric detectors[3] and as ferromagnetic nanotubes.[4] While the structural characterization of vanadium oxide clusters deposited on surfaces[5] has reached atomic resolution, it remains a major experimental challenge in the gas phase.[6] Infrared photodissociation[7] paired with quantum chemistry is currently the most generally applicable approach for cluster ions, but requires intense and tunable infrared radiation sources. In particular in the region below 2000 cm^{-1}, where the fingerprint region of metal oxide clusters is found, only free electron lasers meet these demands.[8]

Herein we report the first experimental infrared spectra of transition metal oxide cluster anions in the gas phase. We combine infrared multiple photon dissociation (IRMPD) spectroscopy with density functional theory (DFT) to characterize the geometric and electronic structure of a representative series of vanadium oxide cluster anions, $(V_2O_5)_n^-$ with n = 2, 3, and 4.[9] Compelling evidence is produced that these anions have the polyhedral cage structures that have been predicted before, but have eluded spectroscopic detection until now.[10, 11] Evidence is also found for a size-induced localization of the extra electron in this series of anions.

((Figure 1))

The IRMPD spectra of mass-selected $V_4O_{10}^-$, $V_6O_{15}^-$ and $V_8O_{20}^-$ are shown on the left in Figure 1. They were measured by irradiating vibrationally cold, mass-selected parent ions with intense, tunable IR radiation from the free electron laser FELIX[12] and monitoring the mass-selected fragment ion yield as a function of laser waverlength. Only when the radiation is resonant with a fundamental vibrational transition can the cluster ions absorb photons, initiating a sequential multiphoton absorption process[13] which leads to heating of the cluster ion and eventually to photodissociation. The simplicity of the $V_4O_{10}^-$ spectrum is striking and immediately suggests a structure of higher symmetry with degenerate transitions. The dominant feature is a single, rather

narrow intense band at 990 cm^{-1}. Based on our previous measurements on vanadium oxide cluster cations it is assigned to vanadyl stretch modes.[14] The weaker signal below 750 cm^{-1} is attributed to V-O-V stretches. The IRMPD spectrum of $V_8O_{20}^-$ is markedly different. While the vanadyl band stays nearly unchanged, a new band, much broader and roughly four times stronger than the vanadyl band, is observed centered at 870 cm^{-1}. The appearance of the $V_6O_{15}^-$ spectrum is intermediate compared to the spectra described above. An intense vanadyl band, somewhat broader and red-shifted, is followed by a for times less intense band at 830 cm^{-1}. No signal is observed below 700 cm^{-1} for the two larger clusters.

((Scheme 1))

To understand these vibrational spectra we performed DFT calculations (B3LYP functional[15, 16]) of cluster geometries and vibrational spectra (see Figure 1, column labeled B3LYP). All three anions are open-shell systems with a single unpaired electron. For $V_4O_{10}^-$ we find a tetragonal D_{2d} structure **(1)** which is minimally Jahn-Teller distorted from the T_d structure. Each vanadium atom is four-fold coordinated, forming one short V=O double bond (159 pm) and three V-O single bonds (181 pm). The four symmetry-equivalent vanadyl bond stretches combine to three IR active b_2 and e modes which are quasi-degenerate and explain the single intense vanadyl band in the IRMPD spectrum. The six symmetric V-O-V bond stretches also give rise to three IR active e and b_2 modes (629 and 609 cm^{-1}, respectively). They have a cumulative oscillator strength that is about 1/3 of the vanadyl bands, in good agreement with experiment. The modes resulting from the six antisymmetric V-O-V bond stretches are below 600 cm^{-1} and have vanishing intensities.

((Scheme 2))

In $V_4O_{10}^-$ the unpaired electron is completely delocalized over d-states of all four vanadium sites as illustrated by its singly-occupied natural orbital **SONO(1)**. In contrast, in the larger anions the unpaired electron localizes at a single vanadium site, which lowers the symmetry of their structures to C_s. For $V_6O_{15}^-$ and $V_8O_{20}^-$ we find the distorted trigonal prism and cube structures **2**

and **3**. Their singly occupied natural orbitals, **SONO(2)** and **SONO(3)**, reflect the localization of the unpaired electron. Compared to $V_4O_{10}^-$, the average V-O(-V) bond distances in $V_8O_{20}^-$ are longer at the electron localization site (189 pm), but shorter at the other sites (177-178pm), while the V=O bond distances are similar and not affected by the localization. Unlike the closed-shell neutral parent compounds, the D_{3h} structure (trigonal prism) of $V_6O_{15}^-$ and the D_{2d} structure (cube) of $V_8O_{20}^-$ are higher order saddle points, 45 and 21 kJ/mol, respectively, above the ground state. For both $V_6O_{15}^-$ and $V_8O_{20}^-$ first order saddle points with C_{2v} symmetry are found 9.8 and 8.7 kJ/mol, respectively, above the ground state. They represent transition structures for the interconversion of two equivalent C_s-minimum structures and have the additional electron delocalized over two sites.

The effects of symmetry breaking are directly observed in the vibrational spectra of these species, indicated by the gray-shaded area in Figure 1. Upon localization of the unpaired electron intense V-O-V stretch transitions appear ~100-200 cm^{-1} below the strong vanadyl band, which replace the weak V-O-V feature more than ~350 cm^{-1} below the vanadyl band in the spectrum of the delocalized case ($V_4O_{10}^-$). The calculated ratio of the cumulative oscillator strengths of the V-O-V modes and the V=O modes is 3.3 for $V_8O_{20}^-$ and 0.3 for $V_4O_{10}^-$, comparing well to the experimental values of 4.4 and 0.4 respectively. The vanadyl modes are not affected by the electron localization and therefore their position and width remain nearly unchanged. Comparison with the experimental infrared spectra confirms the general predictions of the B3LYP model, in particular the pronounced, qualitative changes upon electron localization when the size of the cluster is increased.[17]

Figure 1 shows not only the B3LYP results discussed so far, but also results of DFT calculations which employ the BLYP[16, 18] and BHLYP[16, 19] functionals. The increasing admixture of Fock exchange (zero, 20 % and 50%) in BLYP, B3LYP and BHLYP, respectively, leads to an increasing tendency for symmetry-breaking.[20-22] BHLYP (right column in Figure 1) yields localization of the unpaired electron for all three cage-type anions, also for $V_4O_{10}^-$. Consequently,

the BHLYP spectrum of $V_4O_{10}^-$ shows additional bands between 800 and 900 cm^{-1} that are absent in the experimental spectrum. In contrast, BLYP predicts delocalization of the unpaired electron for all three cage-type anions studied and C_{2v} and D_{2d} structures become the ground states of $V_6O_{15}^-$ and $V_8O_{20}^-$, respectively. All three BLYP spectra do not show any band between 750 and 950 cm^{-1}, which is in clear contrast with the experimental spectra of $V_6O_{15}^-$ and $V_8O_{20}^-$. In summary, Figure 1 shows that only B3LYP reproduces correctly the transition from symmetric (delocalized) to broken-symmetry (localized) structures when passing from $V_4O_{10}^-$ to $V_6O_{15}^-$ in this series of $(V_2O_5)_n^-$ cluster anions.

Figure 2 compares the gas phase IRMPD spectrum of $V_8O_{20}^-$ with the electron energy loss spectrum of a V_2O_5 surface,[23] which also probes vibrational states. The spectra are surprisingly similar in the region above 740 cm^{-1}, both displaying two bands of similar width and relative intensity. Their assignment is identical, i.e., to vibrational modes of singly- and doubly-coordinated oxygen atoms. The third broad band of the surface spectrum is not observed in the gas phase. This can easily be rationalized, because this band is assigned[11, 24] to triply coordinated oxygen sites, which do not exist in the $V_8O_{20}^-$ cluster anion. Hence, the vibrational spectra reflect clearly the common (V=O and V-O-V bonds) and the discriminating (triply coordinated O) structural features of gas phase clusters and solid surfaces.[25][26]

In this communication, the polyhedral cage structures of $(V_2O_5)_n^-$ clusters (n = 2, 3, 4) were identified spectroscopically for the first time using IRMPD. We also found evidence for size-dependent charge localization in these clusters. Symmetry-breaking localization is observed in many other chemical systems for the reverse process, creation of an electron hole.[21] For example, the electron hole created in quartz when doped with Al is not delocalized over all four oxygen sites of the AlO_4 defect site, but localized at one oxygen only.[22] The proper description of electron (hole) localization phenomena by DFT depends on the functional used. In the present case we use the measured IRMPD spectra as criterion for selecting the proper functional and find that only B3LYP has the right admixture of Fock exchange to reproduce the size-dependent change from

delocalized to localized d-electron states in vanadium oxide cages correctly. Even though the largest cluster anion studied here, $V_8O_{20}^-$, is still rather small, it reveals some striking similarities with the properties of a vanadium oxide single crystal surface, making it an interesting gas phase model for surface adsorption and reactivity studies.

Experimental Section

The present experiments were carried out on a previously described tandem mass spectrometer-ion trap system.[27] Vanadium oxide clusters are prepared by pulsed laser vaporization of a vanadium rod in the presence of O_2 seeded in He. The beam of negative ions is collimated and mass-selected in quadrupole mass filter. Mass-selected cluster ions are accumulated and cooled to 15 K in a linear radio-frequency ion trap. IR photodissociation spectra are obtained by photoexcitation of the trapped cold ions with pulsed radiation from the FELIX,[12] and subsequent monitoring of the mass-selective ion yield. A FELIX bandwidth (RMS) of less than 0.3% of the central wavelength and pulse energies of up to 60 mJ per macropulse were used.

Computational Section

Unrestricted Kohn-Sham calculations are made using TURBOMOLE.[28] Triple-zeta valence plus polarization basis sets (TZVP) are applied.[29] Harmonic vibrational frequencies are obtained from second analytic derivatives[30] and were scaled using standard procedures (see supplemental information).

References

[1] B. M. Weckhuysen, D. E. Keller, *Catal. Today* **2003**, *78*, 25-46.

[2] M. S. Whittingham, *Chem. Rev.* **2004**, *104*, 4271-4301.

[3] L. A. L. de Almeida, G. S. Deep, A. M. N. Lima, I. A. Khrebtov, V. G. Malyarov, H. Neff, *Appl. Phys. Lett.* **2004**, *85*, 3605-3607.

[4] L. Krusin-Elbaum, D. M. Newns, H. Zeng, V. Derycke, J. Z. Sun, R. Sandstrom, *Nature* **2004**, *431*, 672-676.

[5] a) J. Schoiswohl, G. Kresse, S. Surnev, M. Sock, M. G. Ramsey, F. P. Netzer, *Phys. Rev. Lett.* **2004**, *92*, 206103; b) N. Magg, B. Immaraporn, J. B. Giorgi, T. Schroeder, M. Bäumer, J. Döbler, Z. L. Wu, E. Kondratenko, M. Cherian, M. Baerns, P. C. Stair, J. Sauer, H.-J. Freund, *J. Catal.* **2004**, *226*, 88-100.

[6] a) A. Dinca, T. P. Davis, K. J. Fisher, D. R. Smith, G. D. Willett, *Int. J. Mass Spectrom.* **1999**, *182/183*, 73-84; b) R. C. Bell, K. A. Zemski, D. R. Justes, A. W. Castleman Jr., *J. Chem. Phys.* **2001**, *114*, 798-811; c) H. J. Zhai, L.-S. Wang, *J. Chem. Phys.* **2002**, *117*, 7882-7888; d) A. Pramann, K. Koyasu, A. Nakajima, K. Kaya, *J. Chem. Phys.* **2002**, *116*, 6521-6528.

[7] M. A. Duncan, *Int. J. Mass Spectrom.* **2000**, *200*, 545-569.

[8] G. von Helden, D. van Heijnsbergen, G. Meijer, *J. Phys. Chem. A* **2003**, *107*, 1671-1688.

[9] A more comprehensive, systematic study of vanadium oxide cluster anions containing two to eight vanadium atoms will be reported elsewhere.

[10] S. F. Vyboishchikov, J. Sauer, *J. Phys. Chem. A* **2000**, *104*, 10913-10922.

[11] S. F. Vyboishchikov, J. Sauer, *J. Phys. Chem. A* **2001**, *105*, 8588-8598.

[12] D. Oepts, A. F. G. van der Meer, P. W. van Amersfoort, *Infrared Phys. Technol.* **1995**, *36*, 297-308.

[13] J. Oomens, G. Meijer, G. von Helden, *J. Phys. Chem. A* **2001**, *105*, 8302-8309.

[14] K. R. Asmis, G. Meijer, M. Brümmer, C. Kaposta, G. Santambrogio, L. Wöste, J. Sauer, *J. Chem. Phys.* **2004**, *120*, 6461-6470.

[15] A. D. Becke, *J. Chem. Phys.* **1993**, *98*, 5648-5652.

[16] C. Lee, W. Yang, R. G. Parr, *Phys. Rev. B* **1988**, *37*, 785-789.

[17] Some discrepancies between experimental and simulated spectra remain and are attributed to the approximate nature of the calculations, which neglect the multiphotonic nature of the absoption process and assume that the potentials are single-well and harmonic.

[18] A. D. Becke, *Phys. Rev. A* **1988**, *38*, 3098-3100.

[19] A. D. Becke, *J. Chem. Phys.* **1993**, *98*, 1372-1377.

[20] C. D. Sherrill, M. S. Lee, M. Head-Gordon, *Chem. Phys. Lett.* **1999**, *302*, 425-430.

[21] M. Sodupe, J. Bertran, L. Rodriguez-Santiago, E. J. Baerends, *J. Phys. Chem. A* **1999**, *103*, 166-170.

[22] G. Pacchioni, F. Frigoli, D. Ricci, J. A. Weil, *Phys. Rev. B* **2001**, *63*, 054102; X. Solans-Monfort, V. Branchadell, M. Sodupe, M. Sierka, J. Sauer, *J. Chem. Phys.* **2004**, *121*, 6034-6041.

[23] B. Tepper, B. Richter, A. C. Dupuis, H. Kuhlenbeck, C. Hucho, P. Schilbe, M. A. bin Yarmo, H.-J. Freund, *Surf. Sci.* **2002**, *496*, 64-72.

[24] V. Brázdová, M. V. Ganduglia-Pirovano, J. Sauer, *Phys. Rev. B* **2004**, *69*, 165420.

[25] In solid compounds, mixed valence polyvanadate species, e.g. $V_{15}O_{36}^{5-}$, are found which also have a cage structure with terminal V=O groups, but contain triply coordinated O in addition to V-O-V bonds. See Ref. 26.

[26] A. Müller, E. Krickemeyer, M. Penk, H.-J. Walberg, H. Bögge, *Angew. Chem., Int. Ed.* **1987**, *26*, 1045-1046.

[27] K. R. Asmis, M. Brümmer, C. Kaposta, G. Santambrogio, G. von Helden, G. Meijer, K. Rademann, L. Wöste, *Phys. Chem. Chem. Phys.* **2002**, *4*, 1101-1104.

[28] a) R. Ahlrichs, M. Bär, M. Häser, H. Horn, C. Kölmel, *Chem. Phys. Lett.* **1989**, *162*, 165-169; b) O. Treutler, R. Ahlrichs, *J. Chem. Phys.* **1995**, *102*, 346-354; c) K. Eichkorn, O. Treutler, H. Öhm, M. Häser, R. Ahlrichs, *Chem. Phys. Lett.* **1995**, *242*, 652-660.

[29] A. Schäfer, C. Huber, R. Ahlrichs, *J. Chem. Phys.* **1994**, *100*, 5829-5835.

[30] P. Deglmann, F. Furche, R. Ahlrichs, *Chem. Phys. Lett.* **2002**, *362*, 511-518.

Figure Captions

Figure 1: Experimental and simulated vibrational spectra of vanadium oxide cluster anions in the region of the V-O single and double bond stretch modes. IRMPD spectra (left) of $V_4O_{10}^-$ (top), $V_6O_{15}^-$ (center) and $V_8O_{20}^-$ (bottom) were measured from 550 to 1175 cm^{-1} monitoring the dominant fragmentation channel, leading to formation of $V_3O_8^-$, $V_4O_{10}^-$, and $V_4O_{10}^-$, respectively. Simulated spectra (right) were obtained from scaled harmonic frequencies and oscillator strengths employing the B3LYP, BLYP, and BHLYP functionals. The calculated stick spectra were convoluted for better comparison with the experiment. Gray shaded peaks indicate localization of the unpaired d-electron (see text).

Figure 2: Vibrational spectra of different forms of vanadium oxide. The IRMPD spectrum of the gas phase cluster anion $V_8O_{20}^-$ (top) and the spectrum of a freshly cleaved 001 surface of V_2O_5 (bottom), measured using high resolution electron energy loss spectroscopy, are shown (see text).

Suggestion for the table of contents

Polyhedral Vanadium Oxide Cages. The first infrared spectra of transition metal oxide cluster anions in the gas phase are reported. In combination with density functional theory they produce compelling evidence that these anions have polyhedral cage structures. With increasing size, the extra electron changes its nature from delocalized to localized which is accompanied by lowering the symmetry of the polyhedra from D_{2d} to C_s.

Keywords

IR spectroscopy, density functional theory, clusters, IRMPD, electron localization

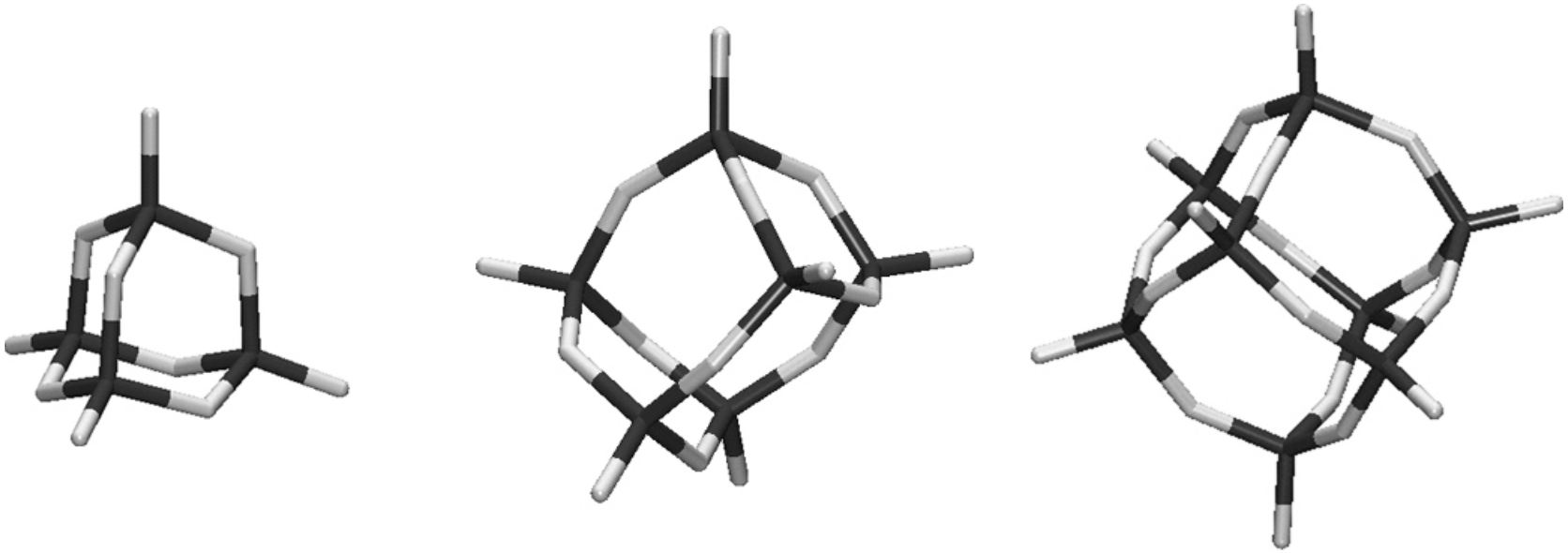

1 **2** **3**

Scheme 1

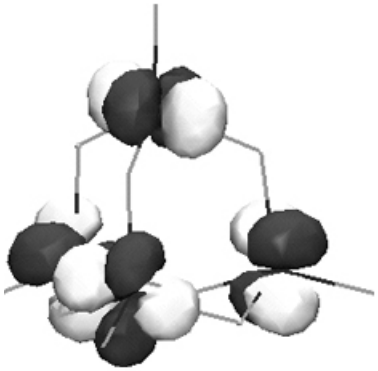

SONO(1)

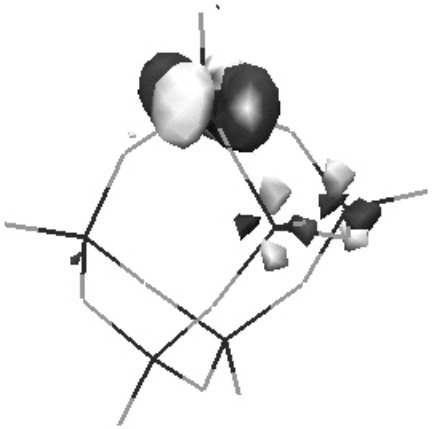

SONO(2)

SONO(3)

Scheme 2

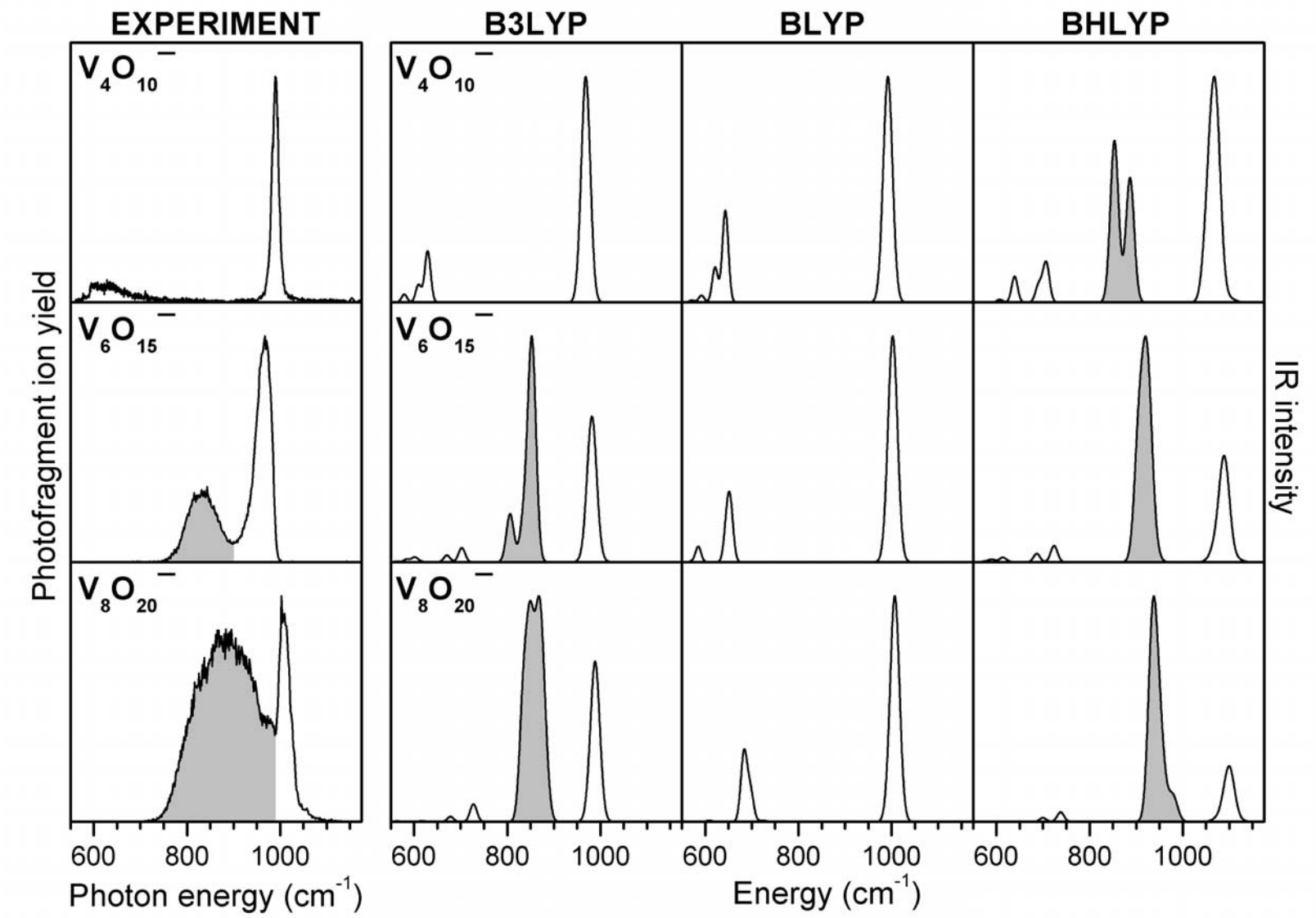
EXPERIMENT
B3LYP
BLYP
BHLYP
$V_4O_{10}^-$
$V_6O_{15}^-$
$V_8O_{20}^-$
Photofragment ion yield
IR intensity
600
800
1000
Photon energy (cm^{-1})
Energy (cm^{-1})

Figure 1

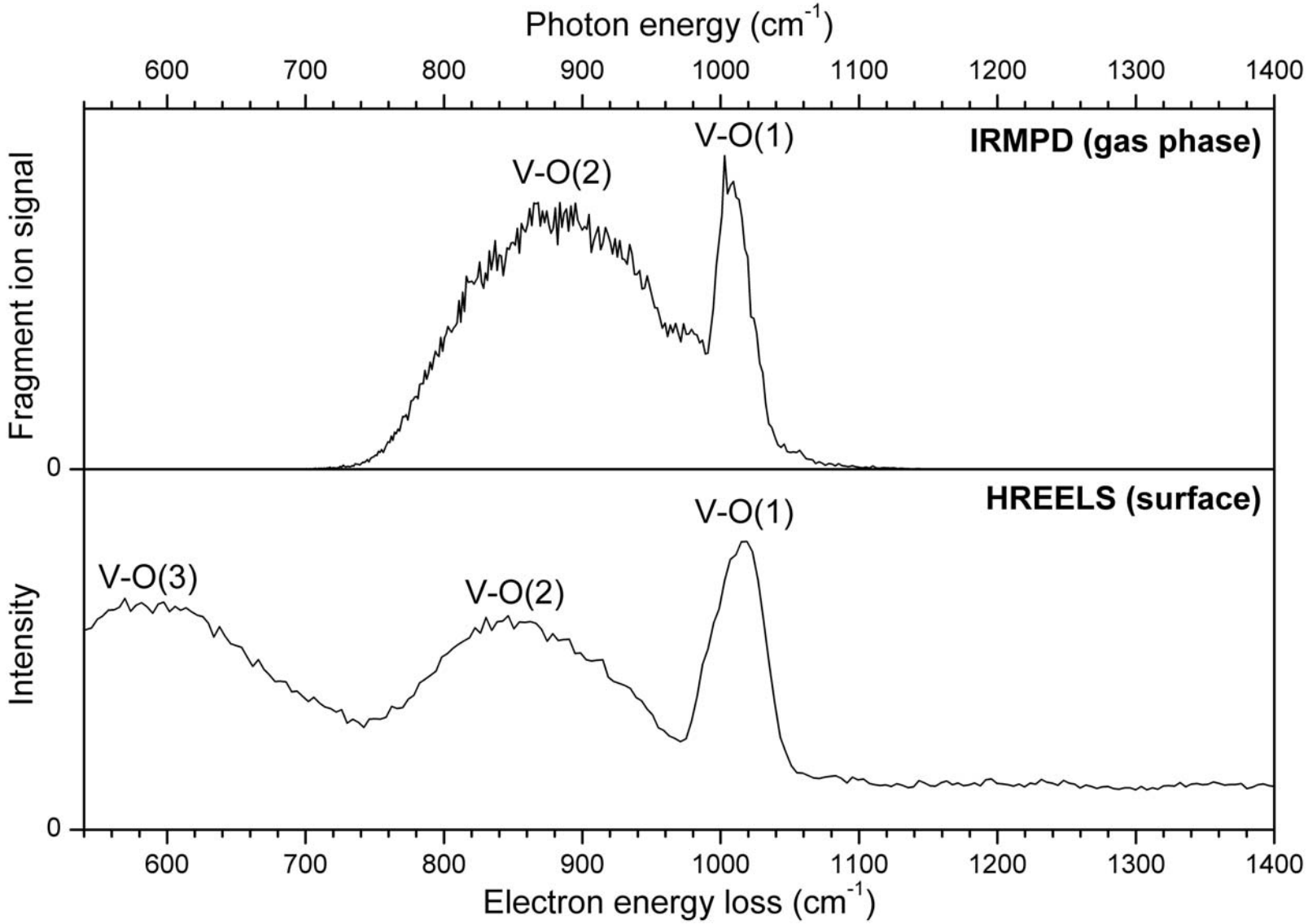
Photon energy (cm-1)
600
700
800
900
1000
1100
1200
1300
1400
Fragment ion signal
0
V-O(1)
V-O(2)
IRMPD (gas phase)
HREELS (surface)
V-O(1)
V-O(3)
V-O(2)
Intensity
0
600
700
800
900
1000
1100
1200
1300
1400
Electron energy loss (cm-1)

Figure 2